



## A Computational Investigation of W-Shaped Transverse Rib on Different Cross Section Roughened Solar Air Heater

Pradeep Kumar Tandan<sup>1</sup> Ashish Muchrikar<sup>2</sup>

<sup>1</sup>PG Scholar, Department of Mechanical Engineering, CIST College Bhopal.

<sup>2</sup>Assistant Professor, Department of Mechanical Engineering, CIST College Bhopal.

### ABSTRACT

Conventional sources of power had been depleting at an alarming price, which makes similarly sustainable achievement of requirement of power very difficult. Thus, warmth switch enhancement era performs an essential function and it's been extensively carried out to many packages as in refrigeration, automotive, procedure enterprise and sun power heater. Convective warmth switch may be superior passively with the aid of using converting waft geometry, or with the aid of using growing warmth switch coefficient among the warmth-shifting floor and the warmth provider fluid. Another opportunity for growing warmth switch to fluid is to rent prolonged surfaces. The use of ribs as fins in a duct will increase the warmth switch region and breaks the laminar sub-layer developing neighbourhood wall turbulence. The warmth switch price is advanced however strain drops is improved as well. A numerical research has been finished to take a look at the results of various rib shapes on warmth switch and fluid waft traits via transversely roughened square channels for Reynolds variety starting from 2300 to 14000 and subjected to uniform warmth flux of  $1500 \text{ W/m}^2$ . Considering single-segment approach, the 3-dimensional continuity, Navier-Stokes, and power equations advanced for the bodily version had been solved with the aid of using the usage of the finite extent method (FVM). The optimization became done with the aid of using the usage of diverse Rib shapes (W-Circular phase rib channel & W-Square phase rib channel) in in-line and special factor ratios ( $D_h=33\text{mm}$ , Aspect ratio of duct  $W/H=8$ , Relative roughness pitch  $P/e=10$ , Relative roughness top  $e/D=0.03375$ ) to attain the most reliable geometry of the rib with most warmth switch price and thermo-hydraulic overall performance parameter (THPP). The maximum THPP became received for the W-Square phase rib at  $Re=2300$  is 1.758. For the W-Square move phase rib channel, the growth in common Nusselt variety price is set 147% extra than the clean channel and evaluate with W-Circular move phase rib channel indicates a better common Nusselt variety round 5.77%.tes a better common Nusselt variety round 5.77%.

Keywords: Artificial Roughness, Solar Air Heater, Roughness Geometry, Nusselt Number, Friction Factor, Thermo Hydraulic Performance, Reynolds Number

### 1. Introduction

The Solar air heater is one of the fundamental gadget via which sun power is transformed into thermal power. Solar air heater is a form of sun thermal machine wherein air is heated in a collector and both transferred at once to the indoors area or to a garage medium. A traditional sun air heater commonly includes an absorber plate, a rear plate, insulation underneath the rear plate, obvious cowl at the uncovered side, and the air flows among the soaking up plate and rear plate. The air receives heated up even as the absorber plate absorbs the heat. The warm air is drawn via the plates with a blower that is operated electrically. The fundamental packages of sun air heater are area heating, seasoning of timber, curing of commercial merchandise and those also can be successfully used for curing/drying of concrete/clay constructing components. The different packages of sun air heater are drying of agro and allied merchandise, meals gadgets including fruits, vegetables, chillies, tea-leaves, fish, salt, etc. The sun air heater may be used in lots of commercial activities (drying/heating) including chemical, pharmaceutical, restricted regions of textiles and hosieries, tannery, safe to eat oil, etc.

## 2. Techniques to Break the Laminar Sub-layer

Employing ribs or grooves at the internal floor of channels has been one of the common passive procedures to interrupt the laminar sub-layer and create neighborhood wall turbulence because of float separation and reattachment among successive corrugations, which reduces the thermal resistance and extensively complements charge of warmth switch. The ribbed channel, due to its effectiveness in warmth switch, is a great candidate for engineering packages, which include move-float warmth exchanger, gas turbine airfoil cooling layout, sun air heater, blade-cooling machine, and gas cooled nuclear reactor.

A lot of research had been executed with inside the literature on artificially roughened surfaces for warmth switch boom however maximum of the research had been mentioned with contrary or all of the 4 partitions roughened for excessive Reynolds range variety with inside the location of gas turbine airfoil cooling machine, gas cooled nuclear reactors, cooling of digital equipment, delivery machineries, combustion chamber liners, missiles, re-access vehicles, deliver hulls and piping networks etc. Several investigators have tried to layout an artificially roughened square duct that could decorate the warmth switch with minimal pumping losses with or 4 roughened surfaces. Artificial roughness with inside the shape of high-quality wires of various shapes and in diverse preparations has been used to create turbulence close to the wall or to interrupt the boundary layer. Various researchers have investigated the outcomes of rib shapes on the warmth switch and friction in a square channel with roughened surfaces. A. Lanjewar, J.L. Bhagoria, R.M. Sarviya [1] synthetic roughness withinside the shape of ribs is a handy approach for boosting thermal overall performance of sun air warmers. This paper offers the experimental research of warmth switch and friction issue traits of a square duct roughened with W-fashioned ribs organized at a bent with admire to the float course on its underside on one vast wall. W ribs had been examined each pointing in downstream W-down and upstream W-as much as the float. The variety of parameters for this have a look at has been determined on the premise of realistic concerns of the machine and working conditions. The duct has a width to peak ratio (W/H) of 8.0, relative roughness pitch (P/E) of 10, relative roughness peak ( $e/D_h$ ) of 0.03375 and attitude of assault of float ( $\alpha$ ) of  $30^\circ$ - $75^\circ$ . The air float charge corresponds to Reynolds range among 2300-14000. The warmth switch and friction issue effects had been as compared with the ones for clean duct below comparable float and thermal boundary situation and thermo-hydraulic overall performance has been investigated. Thermo-hydraulic overall performance evaluation for unique attitude of assault of float indicates that W-down association with attitude of assault of float as  $60^\circ$  offers quality thermo-hydraulic overall performance. In addition warmth switch and friction issue correlations had been evolved. Atul Lanjewar, J.L. Bhagoria, R.M. Sarviya [2] synthetic roughness in shape of ribs is handy approach for enhancement of warmth switch coefficient in sun air heater. This paper offers experimental research of warmth switch and friction issue traits of square duct roughened with W-fashioned ribs on its underside on one vast wall organized at a bent with admire to float course. Range of parameters for this have a look at has been determined on foundation of realistic concerns of machine and working conditions. Duct has width to peak ratio (W/H) of 8.0, relative roughness pitch (p/e) of 10, relative roughness peak ( $e/D_h$ ) 0.018-0.03375 and attitude of assault of float ( $\alpha$ )  $30^\circ$ - $75^\circ$ . Air float charge corresponds to Reynolds range among 2300-14000. Heat switch and friction issue effects had been as compared with the ones for clean duct below comparable float and thermal boundary situation to decide thermo-hydraulic overall performance. Correlations had been evolved for warmth switch coefficient and friction issue for roughened duct. Ahn [3] experimentally investigated the impact of rib shapes on the warmth switch and friction in a rectangular duct. It changed into proven that the triangular-fashioned rib has the very best warmth switch overall performance than some other rib profile for equal rib pitch (P) and rib peak (e). Chandra et al. [4] experimentally investigated the impact of rib shapes on the warmth switch and friction in a rectangular channel. It changed into proven that the rectangular ribs produce better warmth switch augmentation for equal rib pitch (P) and rib peak (e) than some other rib shapes. Liou and Hwang [5] experimentally tested the absolutely evolved turbulent float in a square duct roughened with 3 rib shapes, particularly rectangular, semicircular and triangular move section. The effects confirmed that the for equal rib pitch (P) and rib peak (e) maximum thermal overall performance changed into acquired for the rectangular-ribbed duct and lowest friction issue changed into acquired for the semicircular ribbed duct. But geometric and working parameters applicable to sun air heater are unique from the above cited packages. In the case of sun air warmers, roughness factors should be taken into consideration best on one wall that is the best heated wall comprising the absorber plate. These packages make the fluid float and warmth switch traits notably unique from the ones located in case of roughened partitions and 4 heated wall duct. In the case of sun air warmers, best one wall of the square air passage is subjected to uniform warmth flux whilst the closing 3 partitions are insulated. Literature additionally discovered that the almost maximum appropriate variety of Reynolds range for sun air heater lies among 3800 and 18,000 Kumar and Saini [6] executed a CFD evaluation of fluid float and warmth switch traits of a sun air warmers having arc fashioned rib roughness at the absorber plate. The warmth switch and float evaluation of artificially roughened sun air heater had been executed the usage of 3-d version. FLUENT 6.3.26 business CFD code changed into used as a solver. In order to discover the quality turbulent version, authors examined 4 unique turbulent fashions particularly shear pressure shipping k- $\epsilon$ , preferred k- $\epsilon$ , Renormalization group (RNG) k- $\epsilon$  and realizable k- $\epsilon$  for clean sun air heater. Renormalization group (RNG) k- $\epsilon$  version changed into hired to simulate the fluid float and warmth switch. The effects of the simulation had been correctly established with experimental effects. Overall enhancement ratio with a most price of 1.7 changed into acquired for the roughness geometry similar to relative arc attitude ( $\alpha/90$ ) of 0.333 and relative roughness peak (e/D) of 0.0426 through adopting CFD approach. Gupta et al. [7] suggested that the solar air heater systems operating in a specified range of Reynolds number (3800 -15,000) would show better thermo-hydraulic performance. Bilen and Yapici [8] studied the effect of orientation angle of the turbulence promoters located on the channel wall on the heat transfer. They showed that the highest heat transfer rate is achieved when the promoter orientation angle is 45 degrees. [9] Investigated the air turbulent forced convection heat transfer in a 2-D channel flow over periodic transverse grooves numerically. The grooves were on the lower channel wall subjected to a constant heat flux condition while the upper wall was insulated. The analysis showed that the groove-widths to channel-height ratio of Bill = 0.75 has thermal enhancement factor of about 1.33

II. Nomenclature	
$A_c$	surface area of absorber plate (m <sup>2</sup> )
$C_p$	specific heat of air(J/kg/K)
$D$	equivalent or hydraulic diameter of duct(m)
$E$	rib height(m)
$H$	heat transfer coefficient(W/m <sup>2</sup> /K)
$H$	depth of duct(m)
$I$	turbulence intensity/intensity of solar radiation (W/m <sup>2</sup> )
$K$	thermal conductivity of air(W/m/K)
$L$	length of duct(m)
$L_1$	inlet length of duct(m)
$L_2$	test length of duct(m)
$L_3$	outlet length of duct(m) m mass flow rate(kg/s)
$D_p$	pressure drop(Pa)
$P$	pitch (m) $q_u$ useful heat flux(W/m <sup>2</sup> )
$Q_u$	useful heat gain(W)
$Q_L$	heat loss from collector(W)
$Q_t$	heat loss from top of collector(W)
$T_o$	fluid outlet temperature(K)
$T_i$	fluid inlet temperature(K)
$T_a$	ambient temperature(K)
$T_{pm}$	mean plate temperature(K)
$T_{am}$	mean air temperature(K)
$T_w$	wall temperature(K)
$T_m$	bulk mean temperature(K)
$U_L$	overall heat loss coefficient(W/m <sup>2</sup> /K)
$V$	velocity of air in the duct(m/s)
$W$	width of duct(m)

### 3. Channel Geometry and Boundary Condition

#### Physical Model-

The three-dimensional solar air heater used in the simulations is a rectangular duct with periodically distributed roughness on its upper wall forming the fluid flow. A generic, schematic representation of the rectangular duct.3.1, test, and Fig.3.2 shows the details of the test section. The heat transfer was performed numerically using solar air heater with a rectangular duct height of  $H=25$ mm. The total length of solar air heater duct is  $L=1860$  mm. The length of test section is  $L_2= 1500$  mm, with an upstream (inlet section)  $L_1= 245$  mm to ensure a fully developed flow in the test section. The downstream section (exit section) has the length of  $L_3=115$  mm which is used to prevent the occurrence of adverse pressure effects caused by reversed flow through the computational domain. In this study, the rib height and the rib width are  $e = 1$  mm and  $w =1$  mm, respectively. The dimensions for rectangular case are shown in Fig.3.3 In addition, the heat transfer enhancement is studied as a function of three families, which are represented, by the Reynolds numbers, type of fluid, and rib shapes. W-Circular & W-Square sections of ribs as shown in Fig.3.4 have been investigated in the present work.

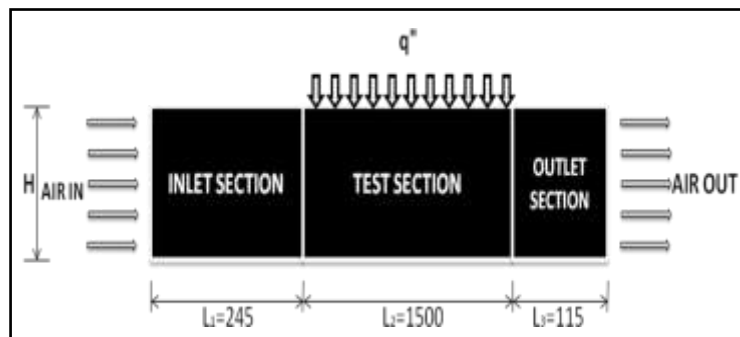


Fig.3.1 Schematic diagram of the investigated region of smooth rectangular channel

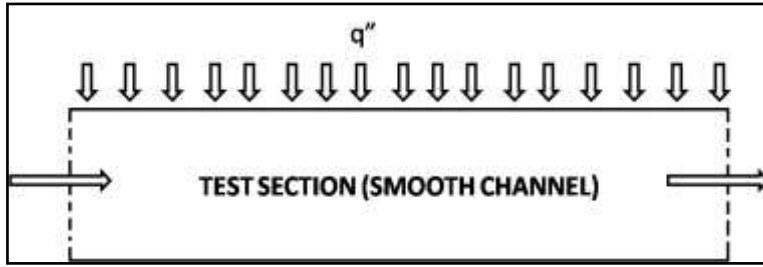


Fig.3.2 Schematic diagram of the investigated region of smooth rectangular channel

**Problem Formulation**

The gift paintings are involved with wearing out third-dimensional simulations on an artificially roughened sun air heater, thru which air flows. The air heater inner floor turned into roughened with the assist of transverse-rectangular and thin (excessive issue ratio) ribs. The ribs have been organized in unique styles particularly one wall only, staggered and in-line on higher face

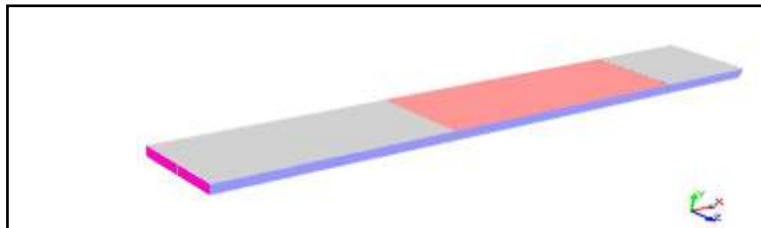


Fig.3.3 Schematic diagram of the investigated region of smooth rectangular channel

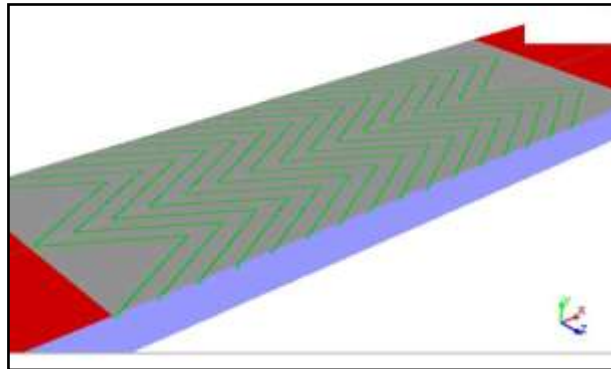


Fig. 3.4.1 Schematic diagram of rib geometry (W-Circular Section Rib)

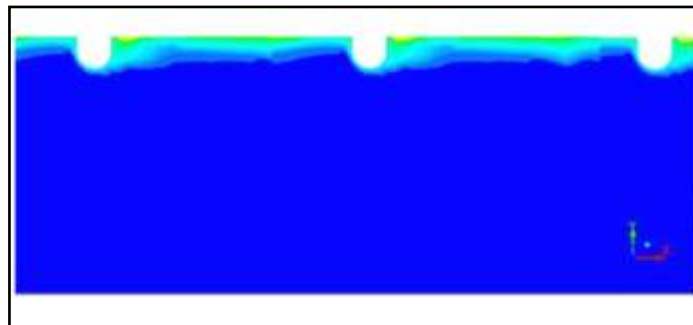


Fig.3.4.2 Sketch of the computational domain of W-Circular Section Rib

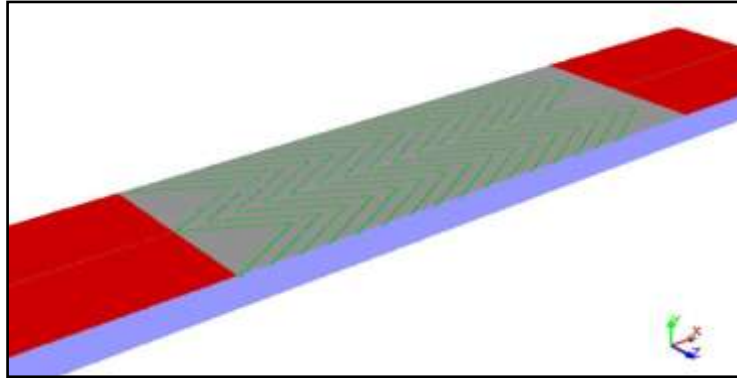


Fig.3.5.1 Schematic diagram of rib geometry (W-Square Section Rib)

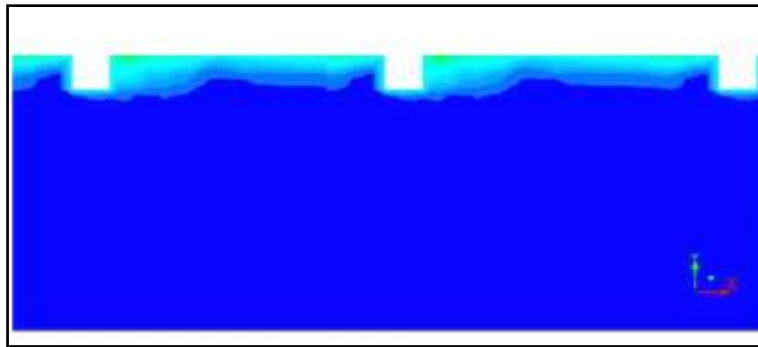


Fig.3.5.2 Sketch of the computational domain of W-Square Section Rib

#### 4. Governing Equation

The consistent three-dimensional shape of the continuity, the time-impartial incompressible Navier Stokes equations and the electricity equation governs turbulent airflow thru artificially roughened sun air heater. These equations may be written as follows: The assumptions made at the working situations of the ribbed channel are as follows:- (1) The ribbed channel operates below consistent-kingdom situations (2) The fluid is incompressible and stays in single-segment alongside the channel (3) The residences of the fluid and channel cloth are impartial of temperature (4) Uniform warmth flux is incident on top wall The single-segment governing equations for waft and warmth switch with inside the ribbed channel may be written with inside the Cartesian tensor device as:-

Continuity equation:

Law of Conservation of Mass: Fluid mass is always conserved. (Equation 1)

$$\frac{\partial(\rho u_i)}{\partial x_i} = 0 \quad (1)$$

Where  $\rho$  is the density of fluid and  $u_i$  is axial velocity

**Momentum equation:**

Newton's 2nd Law: The sum of the forces on a fluid particle is equal to the rate of change of momentum. (Equation 2)

$$\frac{\partial}{\partial x_i}(\rho u_i u_j) = -\frac{\partial p}{\partial x_i} + \frac{\partial}{\partial x_j} \left[ \mu \left( \frac{\partial u_i}{\partial x_j} + \frac{\partial u_j}{\partial x_i} \right) \right] + \frac{\partial}{\partial x_j} (-\rho \overline{u_i u_j}) \quad (2)$$

Here  $\mu$  is the viscosity of fluid,

Where  $\mu$ ,  $u_i$  and  $u_j$  are the fluid viscosity, fluctuated velocity, and the axial velocity, respectively, and the term the turbulent shear stress. The Reynolds-averaged approach to turbulence modeling requires that the Reynolds stresses  $-\rho \overline{u_i u_j}$ , in Eq. (2) needs to be modelled. For closure of the equations, the k- $\epsilon$  turbulence model is chosen. A common method employs the Boussinesq hypothesis to relate the Reynolds stresses to the mean velocity

gradients:

$$-\rho \overline{u_i u_j} = \mu_t \left( \frac{\partial u_i}{\partial x_j} + \frac{\partial u_j}{\partial x_i} \right) \quad (3)$$

### Energy equation:

First Law of Thermodynamics: The rate of heat added to a system plus the rate of work done on a fluid particle equals the total rate of change in energy. (Equation 3)

$$\frac{\partial}{\partial x_i} (\rho u_i T) = \frac{\partial}{\partial x_j} \left[ (\Gamma + \Gamma_t) \frac{\partial T}{\partial x_j} \right] \quad (4)$$

Where  $\Gamma$  and  $\Gamma_t$ , are molecular thermal diffusivity and turbulent thermal diffusivity, respectively and are given by

$$\Gamma = \frac{\mu}{\rho \text{Pr}}, \quad \text{and} \quad \Gamma_t = \frac{\mu}{\rho \text{Pr}_t} \quad (5)$$

The turbulent viscosity term  $\mu_t$  is to be computed from an appropriate turbulence model. The expression for the turbulent viscosity is given as

$$\mu_t = \rho C_\mu \frac{k^2}{\varepsilon} \quad (6)$$

There are two additional equations for the k- $\varepsilon$  turbulent model:

(i) Turbulent kinetic energy (k):

$$\frac{\partial}{\partial x_i} (\rho k u_i) = \frac{\delta}{\delta x_j} \left[ \left( \mu + \frac{\mu_t}{\sigma_k} \right) \frac{\partial k}{\partial x_j} \right] + G_k - \rho \varepsilon \quad (7)$$

(ii) Rate of dissipation ( $\varepsilon$ ):

$$\frac{\partial}{\partial x_i} (\rho \varepsilon u_i) = \frac{\delta}{\delta x_j} \left[ \left( \mu + \frac{\mu_t}{\sigma_\varepsilon} \right) \frac{\partial \varepsilon}{\partial x_j} \right] + C_{1\varepsilon} \frac{\varepsilon}{k} G_k - C_{2\varepsilon} \rho \frac{\varepsilon^2}{k} \quad (8)$$

In the above equation,  $G_k$  represents the rate of generation of the turbulent kinetic energy due to mean velocity gradients while  $\rho \varepsilon$  is its destruction rate. The  $\sigma_k$  and  $\sigma_\varepsilon$  are effective Prandtl numbers for turbulent kinetic energy and rate of dissipation, respectively;  $C_{1\varepsilon}$  and  $C_{2\varepsilon}$  are constants.  $G_k$  is written as:

$$G_k = -\rho u_i u_j \frac{\partial u_j}{\partial x_i} \quad (9)$$

The boundary values for the turbulent quantities near the wall are specified with the enhanced wall treatment method.  $C_\mu=0.09$ ,  $C_{1\varepsilon}=1.44$ ,  $C_{2\varepsilon}=1.92$ ,  $\sigma_k=1.0$ ,  $\sigma_\varepsilon=1.3$  and  $\text{Pr}_t=0.9$  are chosen to be empirical constants in the turbulence transport equations.

The governing equations are solved using a finite volume approach and the SIMPLE algorithm. The solutions are considered to be converged when the normalized residual values reach  $10^{-5}$  for all variables.

### PARAMETERS INVOLVED

To analyze and compare the flow characteristics and heat transfer of different configurations of ribbed channels, following a s:-

(1) Hydraulic diameter ( $D_h$ ):

$$D_h = \frac{4A}{P_h} \quad (10)$$

Where  $A$  is cross-sectional area and  $P_h$  is wetted perimeter of the cross-section

(2) Reynolds number (Re):

$$\text{Re} = \frac{\rho u_m D_h}{\mu} \quad (11)$$

Where  $u_m$  mean velocity of fluid in cross-section here is Reynolds numbers are taken a range of 3800-15000 in order to have turbulent regime.

(3) Nusselt number (Nu):

$$\text{Nu} = \frac{h D_h}{k} \quad (12)$$

Where  $h$  is convective heat transfer co-efficient and  $k$  is thermal conductivity of air

(4) Friction factor for fully developed turbulent flow (f)

The friction factor is computed by pressure drop,  $P$  across the length of test section, and can be obtained by

$$f = \frac{2 \Delta p D}{\rho L u^2} \quad (13)$$

Where  $\Delta p$  is the pressure difference between inlet and outlet:

$$\Delta p = p_{\text{av, inlet}} - p_{\text{av, outlet}} \quad (14)$$

Here,  $p_{\text{av, inlet}}$  and  $p_{\text{av, outlet}}$  are the inlet and outlet average pressure, respectively.

(5) Thermo-hydraulic overall performance parameter (THPP): Under consistent pumping electricity, the thermo hydraulic overall performance parameter has been used to estimate how efficiently an artificially roughened floor complements the warmth switch under consistent pumping electricity constraints.

In order to research basic overall performance of a sun air heater, thermo-hydraulic overall performance need to be evaluated with the aid of using thinking about thermal and hydraulic traits of the sun air heater simultaneously. Webb and Eckert counselled a Thermo hydraulic overall performance parameter that's used to examine the warmth switch of artificially roughened duct to that of a clean duct. A price of thermo hydraulic overall performance parameter more than one guarantees the effectiveness of the usage of an enhancement tool and may be used to examine the overall performance of wide variety of preparations to determine the pleasant amongst these.

$$\text{Thermo hydraulic performance parameter} = \frac{Nu_r/Nu_s}{(f_r/f_s)^{1/3}} \quad (15)$$

Here  $Nu_s$  and  $f_s$  are the Nusselt number and friction factor for smooth channel, respectively and  $Nu_r$  and  $f_r$  are the Nusselt number and friction factor for rough surface with different ribs shape.

### Selection of Appropriate Turbulence Model

Results have been verified with the aid of using evaluating the acquired numerical records with the to be had correlations advanced for a easy channel and additionally with the numerically performed research on transversely roughened channels. First, the Nusselt wide variety and friction element acquired from the existing easy channel for turbulent float are as compared with correlations of Dittus-Boelter and Blasius, respectively. Correlations of Dittus-Boelter:

$$Nu = 0.023Re^{0.8}Pr^{0.4} \quad (\text{for heating}) \quad (16)$$

Correlations of Blasius:

$$f = 0.316Re^{-0.25} \quad \text{for } 3000 < Re < 20000 \quad (17)$$

The Nusselt variety ( $Nu$ ) of channel has been calculated via way of means of the usage of 3 unique turbulence models, including, the usual  $k-\epsilon$  turbulence version, the renormalized group (RNG)  $k-\epsilon$  turbulence version, and the usual  $k-\omega$  turbulence version, and located that the RNG  $k-\epsilon$  turbulence version offers the higher end result of Nusselt variety compared to different turbulence version while as in comparison with the cost of Nusselt variety received from Dittus-Boelter equation.

## 5. Validation of Numerical Method

### 5.1 Validation Of Smooth Model

The gift numerical outcomes on warmth switch and friction traits in a easy wall channel are first established in phrases of Nusselt variety and friction issue. The Nusselt variety and friction issue acquired from the existing easy channel are, respectively, in comparison with the correlations of Dittus-Boelter and Blasius correlation [01] for turbulent glide in duct.

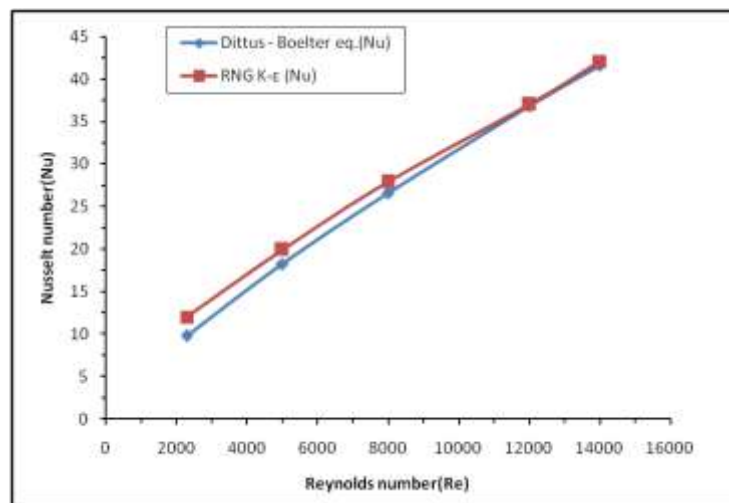


Fig 5.1.1 validation of Nusselt number for smooth channel

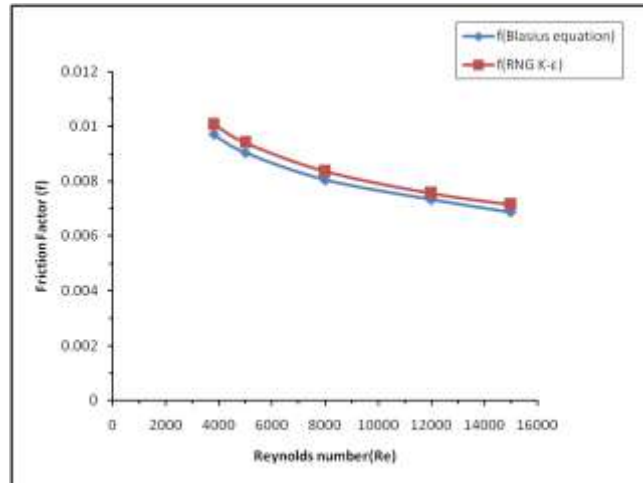


Fig. 5.1.2 validation of friction factor of smooth channel

Fig. 5.1.1 and Fig.5.1.2 display respectively, a evaluation of Nusselt quantity and friction element received from the existing paintings with the ones from correlations of equation (16) and (17). In the figures, the existing results fairly agree nicely within  $\pm 10\%$  for each friction element correlation of Blasius and Nusselt quantity correlation of Dittus-Boelter.

**5.2 RESULT & DISCUSSION**

The results of various rib shapes outfitted in inline, specific rib thing ratios, and Reynolds range at the thermal and waft fields are analysed and mentioned on this segment. The gift numerical outcomes on warmness and waft friction traits in a uniform warmness flux channel ready with 2 mm dimple peak of specific rib shapes (W-Circular segment rib & W-Square segment rib) are offered with inside the shape of Nusselt range and friction factor.

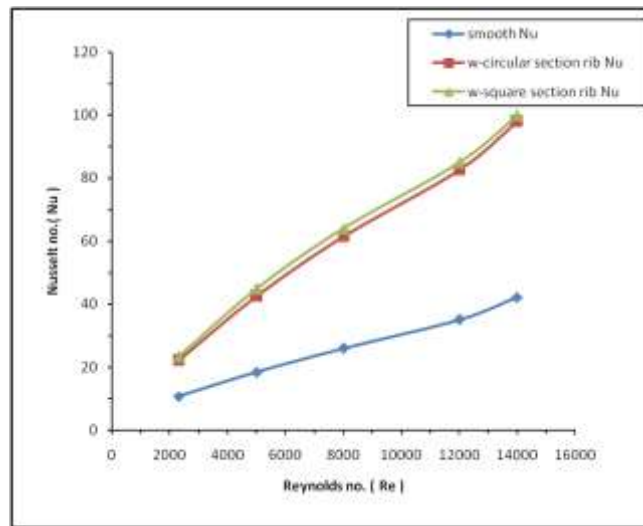


Fig.5.2.1 Variation of Nu number with Reynolds number for various rib shapes

The impact of various dimple shapes has been taken into consideration to study their affect at the thermal and glide fields. The computed common Nusselt wide variety distribution with Reynolds numbers for diverse rib shapes are supplied in Fig.5.2.1 and Table 5.2.1. It may be visible that because the Reynolds wide variety increases, the common Nusselt wide variety additionally increases. The massive Reynolds wide variety is attributed to the better velocity, that can result in disturb the glide, and accordingly the warmth switch is increases. In all cases, the rib channel flows gave better values of Nusselt wide variety than that for easy channel glide because of the induction of excessive re-movement glide and skinny boundary layer with inside the rib channels, main to better temperature gradients. It may be visible in Fig.5.2.1 the rib channel with W-Circular phase rib offers the very best common Nusselt wide variety in any respect Reynolds numbers. Fig5.2.1 indicates that each one the W-Circular phase rib & W-Square phase rib channel yields better common Nusselt wide variety than the easy one for all Reynolds wide variety values. For the W-Circular phase rib & W-Square phase rib channel, the boom in common Nusselt wide variety price is set 107% & 118% at Re=2300, 131% & 144% at Re=5000, 137% & 147% at Re=8000, 136% & 142% at Re=12000, 132% & 137% at Re=14000 greater than the easy channel. The use of the W-Square phase rib channel examine with W-Circular phase rib channel indicates a better common Nusselt wide variety round 05.76% at Re=2300, 05.77% at Re=5000, 04.12% at Re=8000, 02.83% at Re=12000 & 1.92% at Re=14000.



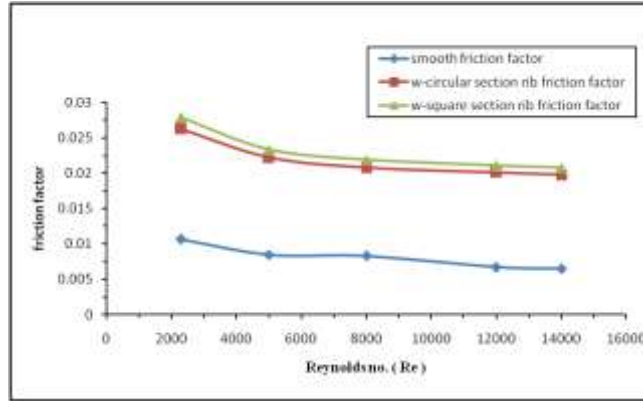


Fig.5.2.2 variation of Friction factor (f) with Reynolds number for various rib shapes

The impact of the usage of the rib turbulators at the isothermal strain drop throughout the examined channel is offered in Fig.five.2.2 and Table five.2.2. The variant of the strain drop is proven in time period of friction element with Reynolds number. In the figure, it's miles obvious that the usage of rib turbulators results in a large boom in friction element over the easy channel. The will increase in friction element for rib turbulators is significantly better than that for the easy channel and is tons better than that during Nusselt number, however. This may be attributed to float blockage, better floor location and the act as a result of the opposite float. As expected, the friction element acquired from the W-Circular phase rib & W-Square phase rib channel is significantly better than that from easy one & the share variant of friction element is 146% & 161% at Re=2300, 162% & 175% at Re=5000, 150% & 163% at Re=8000, 200% & 213% at Re=12000, 206% & 222% at Re=14000 with evaluate to easy channel. The use of the W-Square phase rib channel evaluate with W-Circular phase rib channel suggests a better friction element round 6.16% at Re=2300, five.04% at Re=5000, five.54% at Re=8000, 4.6% at Re=12000 & five.18% at Re=14000. The imply boom in friction element of the usage of the W-Circular phase rib & W-Square phase rib channel one is in a number of five to eight instances over the easy channel. The losses especially come from the dissipation of the dynamical strain of the air because of excessive viscous losses close to the wall, to the more forces exerted with the aid of using opposite float and to better friction of growing floor location and the blockage due to the presence of the ribs.

**5.3 Performance Evaluation**

The Nusselt range ratio,  $Nu_{rib}/Nu_s$ , described as a ratio of common Nusselt range of rib channel to common Nusselt range of clean channel and the fee of ratio plotted towards the Reynolds range fee, is proven in Fig. 5.3.1. In this figure, the Nusselt range ratio has a tendency to lower with the upward thrust of Reynolds range from 2,three hundred to 14,000 for all ribs indicates a barely growth for better Reynolds range fee. The common  $Nu_{rib}/Nu_s$  values for the W-Circular phase rib & W-Square phase rib channel are respectively, around, 2.33, and 2.45 at Re no. 5000.

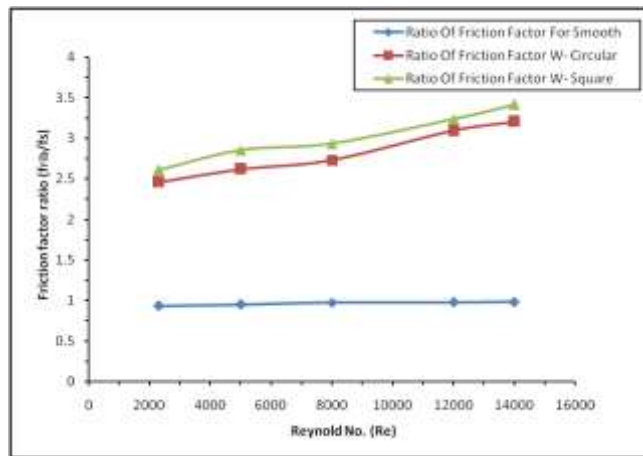


Fig.5.3.2 Variation of friction factor ratio, f(rib)/f(smooth) with Reynolds number

The  $f_r/f_s$  values for the W-Circular section rib & W-Square section rib channel are respectively, around 3.21 and 3.42 at Re=14000. The values of friction factor ratio for all rib shapes are given in table 5.3.2.

Fig.5.3.3 shows the variation of the thermo-hydraulic performance parameter (THPP) with Reynolds number for all rib shapes. For all, the data obtained by measured Nusselt number and friction factor values are compared at a similar pumping power. It is seen in the figure that the thermo-hydraulic performance parameter (THPP) is above unity for all shapes dimple channel when Reynolds number (Re) varies from 2300 to 14,000.

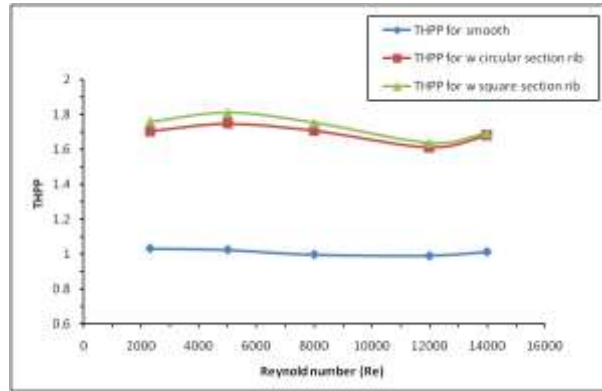


Fig.5.3.3. Variation of thermo-hydraulic performance parameter (THPP) with Reynolds number.

Fig.5.3.3 shows that for each test channel, the values of thermo-hydraulic performance parameter (THPP) have quite similar trend in the considered range of Reynolds number. It is seen that the THPPs for the channels decrease with increasing Reynolds number which means there is an optimum Reynolds number, corresponding to the maximum THPP for each type of geometry. The optimum Reynolds number is related to  $Re = 2300$  for all geometries. The value of THPP index for W-Square section rib channel has been found to be the best among all rib shapes and is about 1.758 at the lowest value of Reynolds number. It also shows that the variation of THPP is high at low Reynolds number but at higher Reynolds number there is low variation in THPP.

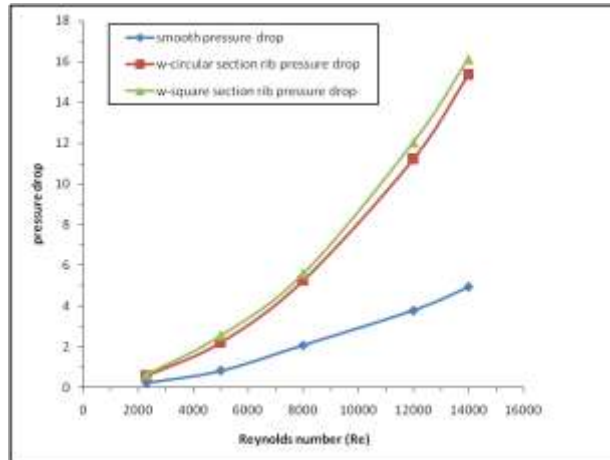


Fig.5.3.4. Variation of Pressure drop with Reynolds number.

Fig.5.3.4 shows that all the W-Circular section rib & W-Square section rib channel yields higher average Pressure drop than the smooth one for all Reynolds number values. The value of Pressure drop is increases with increases in Reynolds no for all geometry ribs and the higher value of Pressure drop is 16.12 at Re no 14000. For the W-Square section channel, the increase in average Pressure drop value is about 400% more than the smooth channel at  $Re=2300$ . The use of the W-Square section rib channel compare with W-Circular section rib channel shows a higher average Pressure drop around 9.73% at  $Re=2300$ .

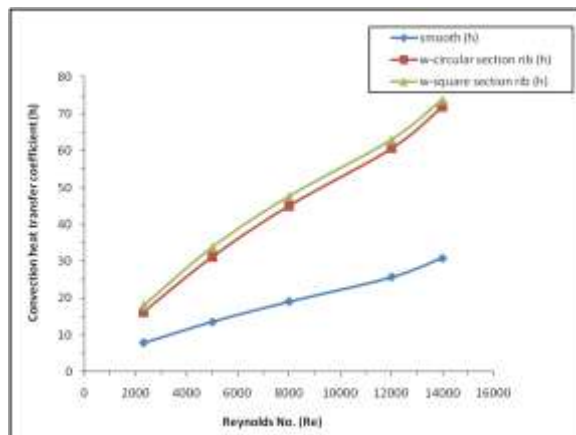


Fig.5.3.5. Variation of Convection heat transfer coefficient (h) with Reynolds no.

Fig5.3.5 shows that all the W-Circular section rib & W-Square section rib channel yields higher Convection heat transfer coefficient (h) than the smooth one for all Reynolds number values. The value of Convection heat transfer coefficient (h) is increases with increases in Reynolds no for all geometry ribs and the higher value of Convection heat transfer coefficient (h) is 73.77 at Re no 14000. For the W-Square section rib channel, the increase in Convection heat transfer coefficient (h) value is about 130.71% more than the smooth channel at Re=2300. The use of the W-Square section channel compare with W-Circular section channel shows a higher Convection heat transfer coefficient (h) around 11.50% at Re=2300.

## 6. Conclusions and Scope For Future Work

### 6.1 Conclusions

In this work, an oblong channel supplied with transversal rib (W-Circular section rib & W-Square section rib) constant heat flux equal of  $1500 \text{ W/m}^2$  has been administered by suggests that of FLUENT 4.5. The aim of the investigation consists into conclude the best form of rib at totally different Sir Joshua Reynolds variety, between 2300 and 14,000, so as to confirm most heat transfer rate and thermo-hydraulic performance parameter (THPP). According to the results

I. Results found from Dittus-Boelter and Blasius equation severally is compared [1] & [2] to validate the turbulence model used for CFD analysis and it's found that Renormalization cluster (RNG) k-epsilon turbulence model results show sensible agreement with the Dittus-Boelter and Blasius empirical correlation results.

II. W-Square section rib channel shows the most average Nusselt variety as compared to alternative rib form channel for all worth of Re from 2300 to 14,000, and its worth is just about a pair of.449 times additional of sleek channel at Re=5,000.

III. W-Square section rib channel shows the most average friction issue as compared to alternative rib form channel for Re vary from 2300 to 14,000, and its worth 3.42 times additional of sleek channel.

IV. In W-Square section rib channel shows most worth of thermo-hydraulic performance parameter (THPP) is one.758, & W-Circular section rib channel of thermo-hydraulic performance parameter (THPP) is one.703, all the worth is found at Sir Joshua Reynolds variety Re=2,300.

V. W-Square section rib channel shows most worth of thermo-hydraulic performance parameter (THPP) is 1.758, for all values of Re from 2300 to 14,000, i.e. W-Square section rib channel exhibits optimum THPP.

VI. For the W-Square section rib, the rise in average Nusselt variety worth is regarding 147% over the sleek channel. The utilization of the W-Square section rib channel compare with W-Circular section rib channel shows the next average Nusselt variety around 5.77%.

VII. For the W-Square section rib channel, the rise in average Pressure drop worth is regarding four-hundredth over the sleek channel at Re=2300. the utilization of the W-Square section rib channel compare with W-Circular section rib channel shows the next average Pressure drop around 9.73% at Re=2300, the rise in Convection heat transfer constant (h) worth is regarding 113.71% over the sleek channel at Re=2300. the utilization of the W-Square section channel compare with W-Circular section rib channel shows the next Convection heat transfer constant (h) around 11.50% at Re=2300.

### 6.2 Scope for Future Work

- Variety of ribs is varied within the rectangular channel to investigate numerically and study the results on the thermal and fluid flow characteristics in flow.
- The transversal rib is organized in staggered kind on each side (top and bottom) of rectangular channel to investigate numerically and study the results of various rib shapes (W-Square section rib, W-Circular section rib), on the thermal and fluid flow characteristics in flow.
- Completely different variety of operating fluid is utilized in the rib form channel to seek out the simplest thermo-hydraulic performance for a given fluid.

## REFERENCES

- [1] A. Lanjewar, J.L. Bhagoria, R.M. Sarviya, Experimental study of augmented heat transfer and friction in solar air heater with different orientations of W-Rib roughness. *Experimental Thermal and Fluid Science* 35 (2011) 986-995.
- [2] Atul Lanjewar, J.L. Bhagoria, R.M. Sarviya, Heat transfer and friction in solar air heater duct with W-shaped rib roughness on absorber plate, *Energy* 36 (2011) 4531-4541. [3] S.W. Ahn, The effect of roughness type on friction factors and heat transfer in roughened rectangular duct, *Int. Commun. Heat Mass Transf.* 28 (7) (2001) 933-942.
- [4] P.R. Chandra, M.L. Fontenot, J.C. Han, Effect of rib profiles on turbulent channel flow heat transfer, *AIAA J. Thermophys. Heat Transf.* 12 (1) (1998) 116-118.

- [5] T.M. Liou, J.J. Hwang, Effect of ridge shapes on turbulent heat transfer and friction in rectangular channel, *Int. J. Heat Mass Transf.* 36 (4) (1993) 931-940.
- [6] Varun, R.P. Saini, S.K. Singal, A review on roughness geometry used in solar air heaters, *Sol. Energy* 81 (2007) 1340-1350.
- [7] D. Gupta, S.C. Solanki, J.S. Saini, Thermo-hydraulic performance of solar air heaters with roughened absorber plates, *Sol. Energy* 61 (1) (1997) 33-42.
- [8] Arulanandam SJ, Hollands KGT, Brundrett E. A CFD heat transfer analysis of the transpired solar collector under no-wind conditions. *Solar Energy* 1999;67(1-3):93-100.
- [9] Ammari HD. A mathematical model of thermal performance of a solar air heater with slats. *Renewable Energy* 2003; 28:1597-615.
- [10] Chaube A, Sahoo PK, Solanki SC. Analysis of heat transfer augmentation and flow characteristics due to rib roughness over absorber plate of a solar air heater. *Renewable Energy* 2006;31:317-31.
- [11] Chaube A, Sahoo PK, Solanki SC. Effect of roughness shape on heat transfer and flow friction characteristics of solar air heater with roughened absorber plate. *WIT Transactions on Engineering Sciences* 2006;53: 43-51.
- [12] Wang C, Guan Z, Zhao X, Wang D. Numerical simulation study on transpired solar air collector. In: *Proceedings of the sixth international conference for enhanced building operations*, 6-9 November 2006, Shenzhen, China; 2006.
- [13] Varol Y, Oztop HF. A comparative numerical study on natural convection in inclined wavy and flat-plate solar collectors. *Building and Environment* 2008; 43: 1535-44.
- [14] Kumar S, Saini RP. CFD based performance analysis of a solar air heater duct provided with artificial roughness. *Renewable Energy* 2009; 34:1285-91.
- [15] Karmare SV, Tikekar AN. Analysis of fluid flow and heat transfer in a rib grit roughened surface solar air heater using CFD. *Solar Energy* 2010; 84:409-17.
- [16] Soi A, Singh R, Bhushan B. Effect of roughness element pitch on heat transfer and friction characteristics of artificially roughened solar air heater duct. *International Journal of Advanced Engineering Technology* 2010;1(3): 339-46.
- [17] Giri AK. CFD analysis of reattachment point, heat transfer and fluid flow of a solar air heater duct provided with artificial roughness. M.Tech. dissertation. MANIT Bhopal, India; 2010.
- [18] Rajput RS. Heat transfer and fluid flow analysis of inverted U-type turbulator in a solar air heater duct by CFD. M.Tech. dissertation. MANIT Bhopal, India; 2010.
- [19] Sharma S, Singh R, Bhushan B. CFD based investigation on effect of roughness element pitch on performance of artificially roughened duct used in solar air heaters. *International Journal of Advanced Engineering Technology* 2011;2(1): 234-41.
- [20] Sharma AK, Thakur NS. CFD based fluid flow and heat transfer analysis of a v- shaped roughened surface solar air heater. *International Journal of Advanced Engineering Technology* 2012; 4(5):2115-21.
- [21] Gandhi BK, Singh KM. Experimental and numerical investigations on flow through wedge shape rib roughened duct. *The Institution of Engineers (India) Journal—MC* 2010; 90:13-8 January.